Article
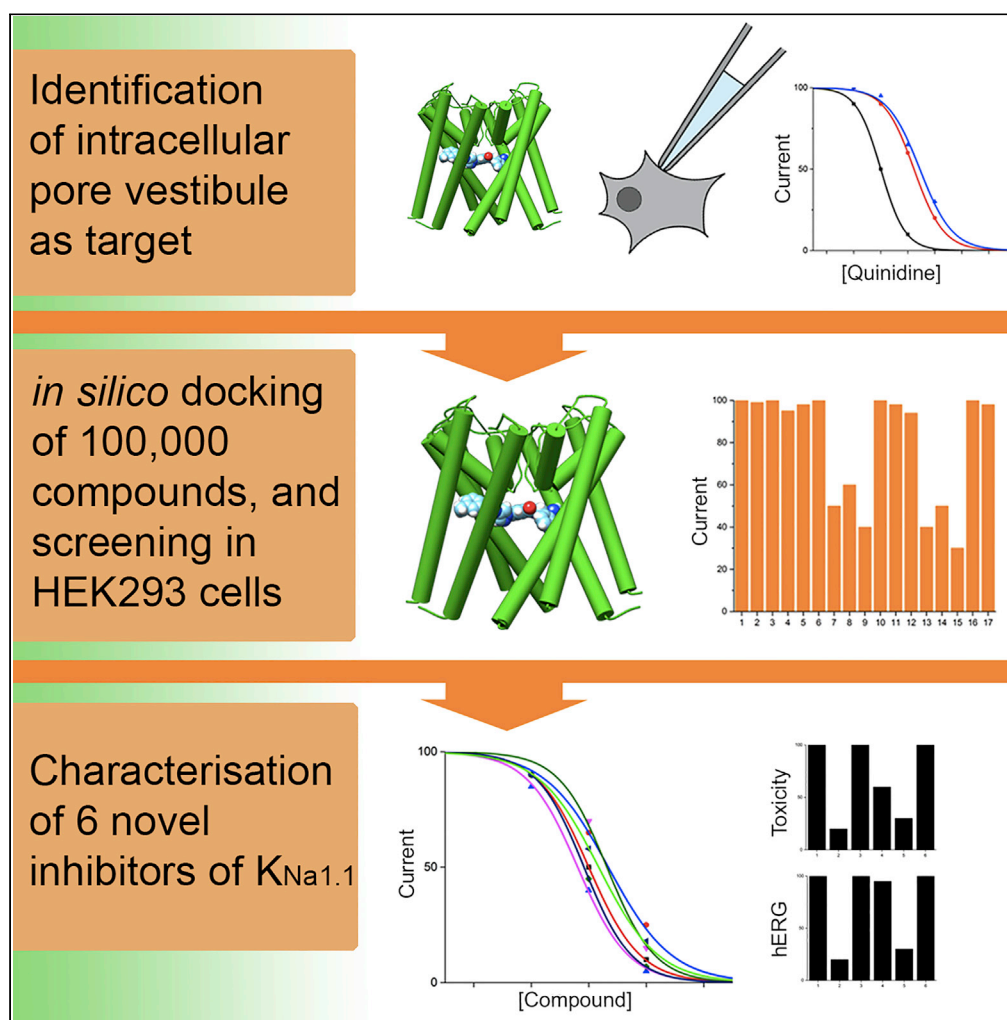
Structure-Based Identification and Characterization of Inhibitors of the Epilepsy-Associated $K_{Na}1.1$ (KCNT1) Potassium Channel

Identification of intracellular pore vestibule as target

in silico docking of 100,000 compounds, and screening in HEK293 cells

Characterisation of 6 novel inhibitors of $K_{Na}1.1$

Bethan A. Cole, Rachel M. Johnson, Hattapark Dejakaisaya, Nadia Pilati, Colin W.G. Fishwick, Stephen P. Muench, Jonathan D. Lippiat

j.d.lippiat@leeds.ac.uk

HIGHLIGHTS

$K_{Na}1.1$ potassium channel inhibitors work by blocking the channel pore

A chicken $K_{Na}1.1$ cryo-EM structure was used for virtual compound screening

Six novel inhibitors of human $K_{Na}1.1$ channels were identified

Inhibitors may help develop treatments for human *KCNT1* gain-of-function disorders

Article

Structure-Based Identification and Characterization of Inhibitors of the Epilepsy-Associated K$_{Na}$1.1 (KCNT1) Potassium Channel

Bethan A. Cole,[1] Rachel M. Johnson,[1,2,5] Hattapark Dejakaisaya,[1,6] Nadia Pilati,[3] Colin W.G. Fishwick,[2,4] Stephen P. Muench,[1,2] and Jonathan D. Lippiat[1,7,*]

SUMMARY

Drug-resistant epileptic encephalopathies of infancy have been associated with *KCNT1* gain-of-function mutations, which increase the activity of K$_{Na}$1.1 sodium-activated potassium channels. Pharmacological inhibition of hyperactive K$_{Na}$1.1 channels by quinidine has been proposed as a stratified treatment, but mostly this has not been successful, being linked to the low potency and lack of specificity of the drug. Here we describe the use of a previously determined cryo-electron microscopy-derived K$_{Na}$1.1 structure and mutational analysis to identify how quinidine binds to the channel pore and, using computational methods, screened for compounds predicated to bind to this site. We describe six compounds that inhibited K$_{Na}$1.1 channels with low- and sub-micromolar potencies, likely also through binding in the intracellular pore vestibule. In hERG inhibition and cytotoxicity assays, two compounds were ineffective. These may provide starting points for the development of new pharmacophores and could become tool compounds to study this channel further.

INTRODUCTION

Gain-of-function mutations in the *KCNT1* gene are associated with severe, drug-resistant forms of childhood epilepsy (Barcia et al., 2012; Heron et al., 2012). Epilepsy of infancy with migrating focal seizures (EIMFS) and autosomal dominant nocturnal frontal lobe epilepsy (ADNFLE) were the first disorders found to be associated with *KCNT1*, with the more recently described Ohtahara syndrome (Martin et al., 2014), West syndrome (Ohba et al., 2015), Lennox-Gastaut syndrome (Jia et al., 2019), and sleep-related hypermotor epilepsy (Cataldi et al., 2019; Rubboli et al., 2019). In addition to frequent seizures, patients may also present developmental delay and psychiatric and intellectual disabilities (Gertler et al., 2018; Lim et al., 2016). *KCNT1* encodes a sodium-activated potassium channel subunit, K$_{Na}$1.1, which has previously been termed SLACK and Slo2.2 (Joiner et al., 1998; Yuan et al., 2003). Similar to other potassium channels, the functional proteins are formed by a tetramer of subunits, each of which possesses six transmembrane alpha helices, a re-entrant pore loop between the fifth and sixth helix that forms the selectivity filter, and two intracellular regulation of conductance of potassium (RCK) domains (Hite et al., 2015). K$_{Na}$1.1-containing channels are expressed throughout the central nervous system (Bhattacharjee et al., 2002; Rizzi et al., 2016) and are believed to have a stabilizing effect on the membrane potential following sodium influx during neuronal excitation (Budelli et al., 2009; Cervantes et al., 2013; Hage and Salkoff, 2012; Liu and Stan Leung, 2004; Nanou et al., 2008). Virtually all epilepsy-associated *KCNT1* mutations increase channel activity, although why epilepsy should arise is not understood, since potassium channel opening is usually associated with a decrease in neuronal excitability. One proposed mechanism, based on studies of human stem cell-derived neurons harboring one such mutation, is that hyperexcitability can be caused by an enhanced sodium-dependent after-hyperpolarization, facilitating an increase in the rate of action potential firing (Quraishi et al., 2019).

Quinidine is a class I antiarrhythmic agent, which exerts its effects by non-selectively inhibiting cardiac cation channels at micromolar concentrations. Notably, quinidine also inhibits K$_{Na}$1.1 channels (Yang et al., 2006), including those harboring epilepsy-causing mutations, at similar concentrations, leading to

[1]School of Biomedical Sciences, Faculty of Biological Sciences, University of Leeds, Leeds LS2 9JT, UK

[2]Astbury Centre for Structural Molecular Biology, University of Leeds, Leeds LS2 9JT, UK

[3]Autifony Srl, Istituto di Ricerca Pediatrica Citta' della Speranza, Corso Stati Uniti, 4f, 35127 Padova, Italy

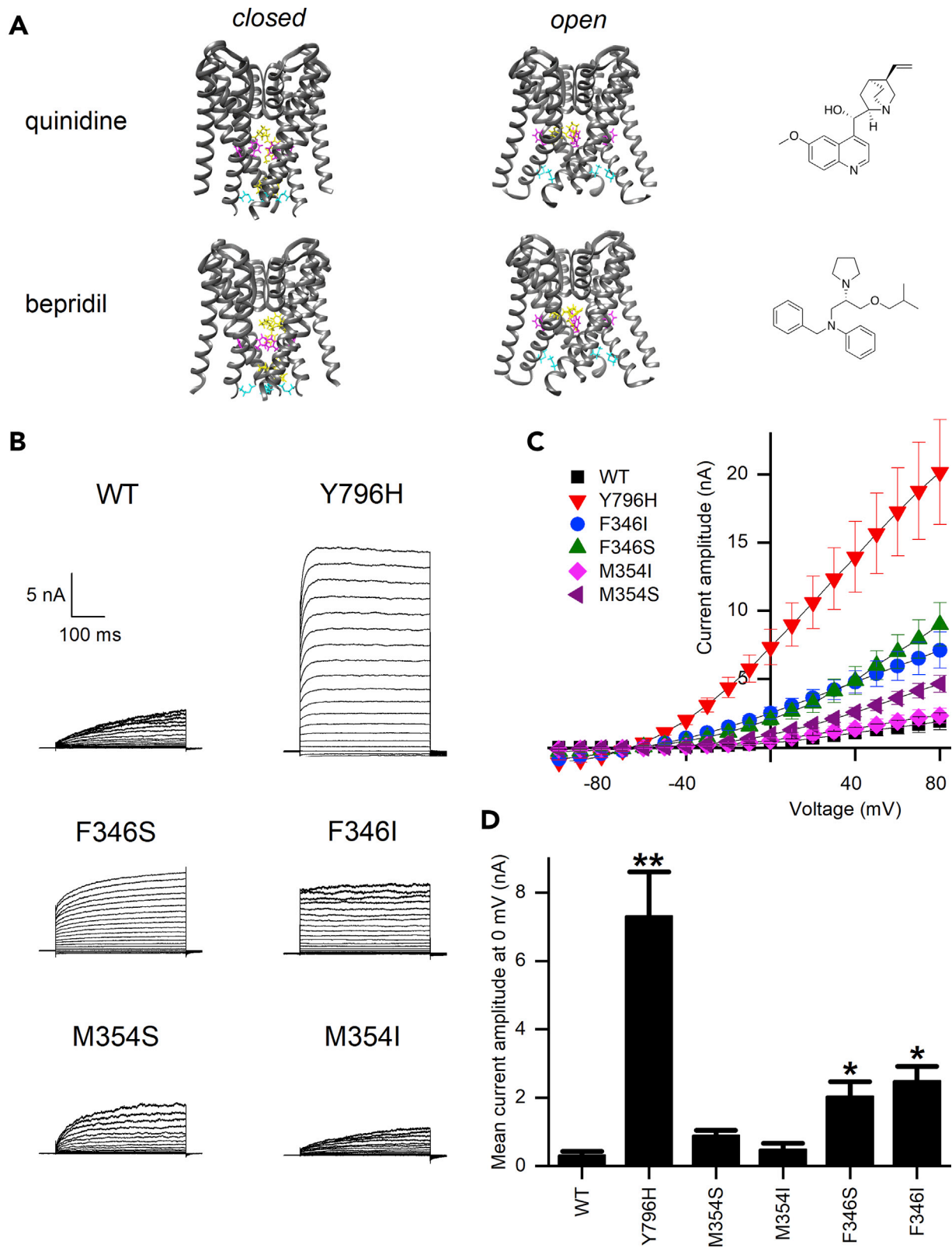[4]School of Chemistry, University of Leeds, Leeds LS2 9JT, UK

[5]Present address: Monash Institute of Pharmaceutical Sciences, Monash University, 399 Royal Parade, Parkville, VIC 3052, Australia

[6]Present address: Department of Neuroscience, Monash University, Melbourne, VIC 3004, Australia

[7]Lead Contact

*Correspondence:
j.d.lippiat@leeds.ac.uk

https://doi.org/10.1016/j.isci.2020.101100

A

closed   open

quinidine

bepridil

B

WT   Y796H

5 nA
100 ms

F346S   F346I

M354S   M354I

C

- ■ WT
- ▼ Y796H
- ● F346I
- ▲ F346S
- ◆ M354I
- ◄ M354S

Current amplitude (nA)

Voltage (mV)

D

Mean current amplitude at 0 mV (nA)

WT   Y796H   M354S   M354I   F346S   F346I

Figure 1. Molecular Docking of Inhibitors and Functional Analysis of Mutant K$_{Na}$1.1 Channels Used in This Study

(A) Docking of quinidine and bepridil (yellow) into the K$_{Na}$1.1 pore domain, comprising the S5, P loop, and S6 of the closed and open conformational states (gray); side chains equivalent to F346 (magenta) and M354 (cyan) of the human K$_{Na}$1.1 homolog are indicated.

(B and C) (B) Representative whole-cell currents and (C) mean ($\pm$SEM, n = 5–9 cells) current-voltage plots from non-transfected (NT) HEK 293 cells and cells transfected with wild-type (WT), pore mutant (F346S, F346I, M354S, M354I), or disease-causing mutant (Y796H) K$_{Na}$1.1.

(D) Mean current amplitude at 0 mV from the data in (C); *p < 0.05, **p < 0.005 compared with WT, independent one-way ANOVA with Games-Howell post hoc test.

the hypothesis that quinidine could reverse the gain of function and treat *KCNT1*-associated epilepsy (Mikati et al., 2015; Milligan et al., 2014). Limited improvement has been achieved in a small number of patients using quinidine therapy, but in the majority of cases it is ineffective (Chong et al., 2016; Fitzgerald et al., 2019; Madaan et al., 2018; McTague et al., 2018; Mikati et al., 2015; Mullen et al., 2018). The lack of selectivity and low potency of quinidine in inhibiting K$_{Na}$1.1 channels, with IC$_{50}$ values in the order of 0.1 mM (Rizzo et al., 2016; Yang et al., 2006), in the central nervous system without significantly affecting cardiac function is a concern and limits the dosing levels of quinidine (Mullen et al., 2018). Moreover, there is still a paucity of information on the binding site and the mode of action of K$_{Na}$1.1 inhibitors. Other reported inhibitors of K$_{Na}$1.1 are bepridil (Yang et al., 2006) and clofilium (de Los Angeles Tejada et al., 2012), both of which also have inhibitory effects on cardiac cation channels. The identification of alternative drugs that better target K$_{Na}$1.1 are therefore desired (Mikati et al., 2015; Milligan et al., 2014). The mechanisms by which these three drugs inhibit potassium channels, hERG in particular, have been studied previously and involve direct block of the pore via the intracellular vestibule and are coordinated by aromatic side-chains, such as phenylalanine (Kamiya et al., 2006; Knape et al., 2011; Macdonald et al., 2018; Perry et al., 2004; Wrighton et al., 2015).

With the development of direct electron detectors, more powerful microscopes, and improved data processing software, there has been an expansion of the use of cryo-electron microscopy (cryo-EM) and single particle analysis to determine high-resolution structures of membrane proteins (Rawson et al., 2016). Bypassing the need to crystallize membrane protein samples makes this approach particularly attractive. One of the first high-resolution ion channel structures determined by cryo-EM was the chicken K$_{Na}$1.1 channel, initially described at 4.5 Å resolution (Hite et al., 2015), with the inactive and activated conformations subsequently resolved to 4.3 and 3.8 Å, respectively (Hite and MacKinnon, 2017). The increase in resolution enables the generation of molecular models, which presents new opportunities that can be utilized in computer-aided drug discovery (CADD) or *in silico* drug design. To discover new therapies for rare disorders, such as those caused by *KCNT1* mutations, efficiencies of drug development cost and time are required (Swinney and Xia, 2014). Computer-aided approaches, such as virtual screening, can help reduce the need for functional screening of large compound sets by predicating which chemicals are likely to occupy a defined binding site (Lin et al., 2020).

In this study, we used the cryo-EM-derived structures of the K$_{Na}$1.1 channel to model quinidine binding *in silico*, having hypothesized that it blocks the channel pore, similar to its interaction with hERG. Having identified the intracellular pore vestibule as the likely site for known inhibitors to bind, we then conducted virtual high-throughput screening of a library of commercially available compounds with the view of identifying more potent and selective binders. We now report the identification of six diverse compounds that inhibit K$_{Na}$1.1 more potently than the quinidine.

RESULTS

Identification of Inhibitor Binding Site in the K$_{Na}$1.1 Channel Pore

In the absence of potent and selective inhibitors of K$_{Na}$1.1 potassium channels, we sought to use computational approaches to identify inhibitors with improved properties. To identify a region in the K$_{Na}$1.1 structure to focus *in silico* screening, we first sought to identify how compounds known to inhibit the channel exert their effects. Hypothesizing that both quinidine and bepridil inhibit channels by occupying the inner pore vestibule we created a minimal structural model of the channel pore by removing the S1 to S4 and the cytosolic domains of the cryo-EM structures of the "closed" and "open" chicken K$_{Na}$1.1 channel (Hite and MacKinnon, 2017). This left the S5, pore loop, and S6 of each subunit, which is highly conserved between chicken and human K$_{Na}$1.1. Using automated procedures, both inhibitors were docked into the pore in its closed conformation at two distinct sites: in the vicinity of the equivalent positions of F346 and M354 in the S6 segment of the human isoform (Figure 1A). In contrast, using the model of the open conformation,

A

B

C
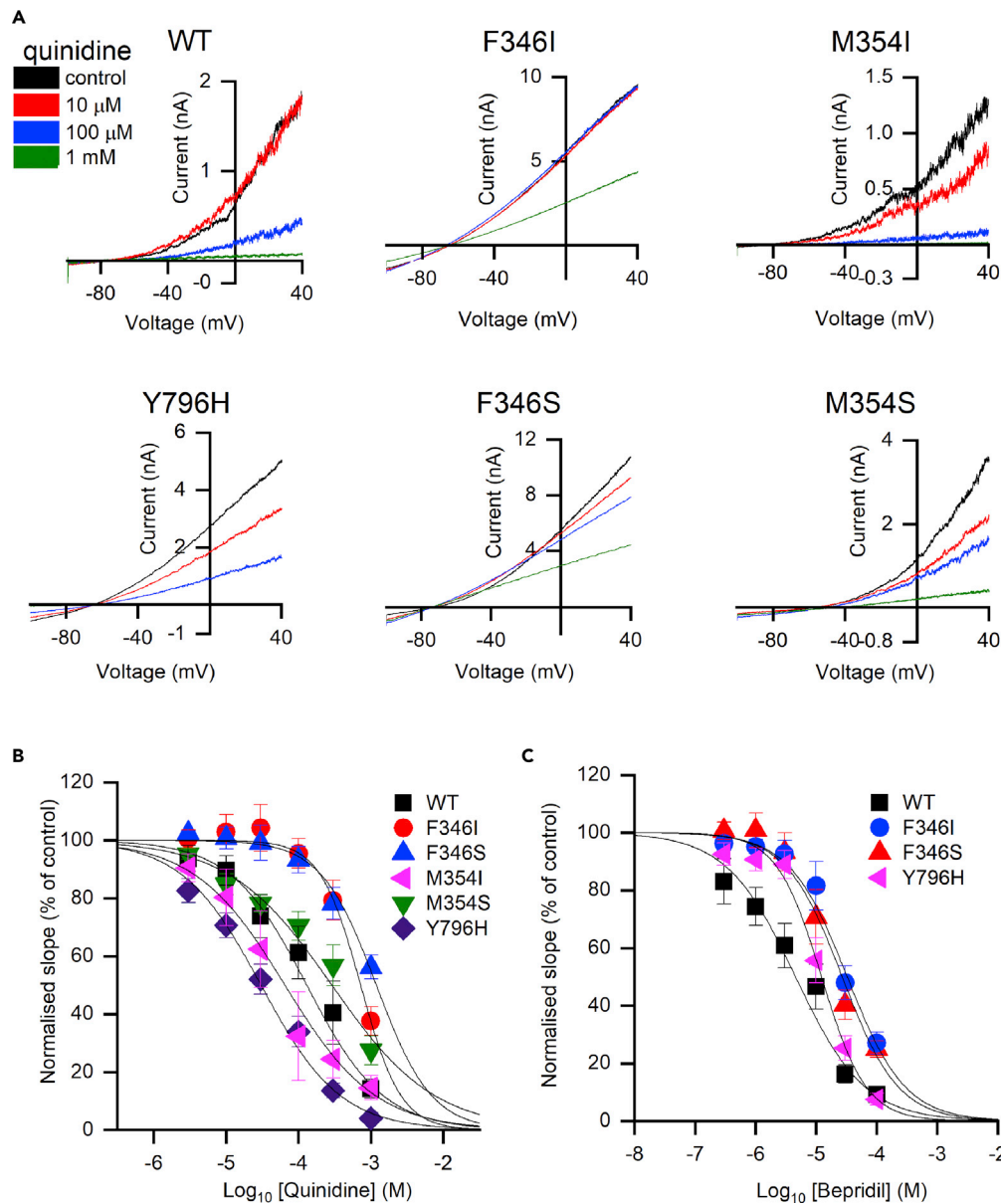
Figure 2. Concentration-Inhibition Analysis of Wild-Type and Mutant $K_{Na}1.1$ Channels by Quinidine and Bepridil

(A) Representative currents evoked by voltage ramps from cells expressing WT or mutant $K_{Na}1.1$ with increasing concentrations of quinidine as indicated.

(B) Mean ($\pm$SEM) concentration-inhibition plots for wild-type and mutant $K_{Na}1.1$ channels in response to 3 μM to 1 mM quinidine. Mean ($\pm$SEM) IC_{50} for WT, 124.99 $\pm$ 34.52 μM (n = 5 cells); F346I, 736.08 $\pm$ 94.09 μM (n = 5); F346S, 1.23 $\pm$ 0.19 mM (n = 4); M354I, 99.23 $\pm$ 49.61 (n = 5); M354S, 247.16 $\pm$ 19.96 μM (n = 5); Y796H, 38.00 $\pm$ 12.89 μM (n = 5).

(C) Mean ($\pm$SEM) concentration-inhibition plots for wild-type and mutant $K_{Na}1.1$ channels in response to 0.3–100 μM bepridil. IC_{50} for WT, 6.36 $\pm$ 2.12 μM (n = 5); F346I, 35.91 $\pm$ 11.01 μM (n = 4); F346S, 23.43 $\pm$ 5.17 μM (n = 5).

quinidine and bepridil could only be docked to the site involving F346 (Figure 1A). To validate the docking, both residues (F346 and M354) of human $K_{Na}1.1$ were mutated to isoleucine and serine (Figures 1B and 1C) and inhibition by quinidine and bepridil was evaluated further. Mutation of M354 had modest effects, with no significant effect on potency of quinidine, but the mutation of F346 to I346 reduced the potency approximately 10-fold (Figure 2). We found that mutating these pore residues, particularly F346, also increased channel activity, with respect to current amplitude and reduced current rectification (Figures 1B–1D). To exclude the possibility that increased channel activity was not the cause of the reduced efficacy of the

inhibitors, for example, through preferential block of the closed state, their effects on a disease-causing gain-of-function mutation, Y796H (Heron et al., 2012), was explored. This mutation causes an amino acid substitution in a $K_{Na}1.1$ intracellular region distal to the pore domain and caused a large increase in $K_{Na}1.1$ channel activity (Figures 1B–1D). In contrast to the pore mutants, quinidine inhibited this mutant channel with a 3-fold increase in potency (Figure 2B).

Virtual Screening and Validation of $K_{Na}1.1$ Inhibitors

Having identified the internal vestibule, just below the selectivity filter, as the likely site for inhibitor binding, we used this region in the minimal pore structure of the open channel conformation to dock compounds using *in silico* screening and a diverse library of 100,000 drug-like molecules. This approach was complemented by computational identification of compounds with structural similarity to bepridil, the most potent of the known inhibitors of $K_{Na}1.1$, and then also docking these compounds into the structure of the $K_{Na}1.1$ channel pore. Both computational techniques resulted in a list of compounds, ranked by their docking score and predicted binding affinities. A selection of 17 compounds (details in Table S1), based on their ranking and commercial availability, were then obtained and evaluated for their ability to inhibit human $K_{Na}1.1$ channels expressed in HEK cells. At 10 μM, six of the compounds inhibited $K_{Na}1.1$ currents by at least 40% and were selected for further analysis (Figure 3A). Initially, and to validate inhibition in the inner pore vestibule, we tested the ability of these compounds to inhibit F346S $K_{Na}1.1$, which had showed reduced sensitivity to both quinidine and bepridil. At 10 μM, the degree by which F346S $K_{Na}1.1$ was inhibited by each compound was reduced, compared with WT $K_{Na}1.1$ (Figure 3A). Concentration-inhibition analysis (Figures 3B–3D) yielded mean IC_{50} concentrations ranging from 0.6 to 7.4 μM with WT $K_{Na}1.1$. In comparison, quinidine and bepridil inhibited WT $K_{Na}1.1$ with IC_{50} values in the order of 125 μM and 6.4 μM, respectively (Figures 2 and 3D). Inspection of the inhibitors docked into the $K_{Na}1.1$ pore domain suggests that binding involves both hydrophobic interactions with S6 pore-lining residues and hydrogen-bonding with P loop residues (Figure 4 and Table S1).

The nature of the inhibition by these compounds was explored further. To be used therapeutically, $K_{Na}1.1$ inhibitors would be required to inhibit channels that have epilepsy-causing amino acid substitutions. We therefore explored the potency of the inhibitors with Y796H $K_{Na}1.1$ gain-of-function mutation. Each of the six compounds inhibited the mutant channels, but in this experiment BC7 and BC14 were significantly less potent (Figures 3B–3D and S1). We also explored the importance of chemical groups in channel inhibition, using BC12 as an example, for which several analogues were commercially available. Each analogue failed to reduce WT $K_{Na}1.1$ channel currents by more than approximately 10% at 10 μM and were deemed inactive (Figure S2).

Preliminary Toxicological Assessment of $K_{Na}1.1$ Channel Inhibitors

Finally, to anticipate toxicological effects of these compounds, should they or derivatives be developed further, we studied their effects on hERG potassium currents and in a cellular toxicity assay. From measurements of tail current amplitudes, 10 μM BC5, BC6, and BC7 almost completely inhibited hERG channels expressed in HEK 293 cells (>80%, Figures 5A and 5B). In contrast, BC14 had a partial effect (approximately 45%) at the same concentration, whereas BC12 and BC13 were even less effective, reducing currents by approximately 10%–20%. In cytotoxicity assays, which involved exposing HEK 293 cells to compounds for 24 h, only BC7 exhibited a concentration-dependent reduction in cell viability, at concentrations of 1 μM and above (Figure 5C). With BC5, B6, and BC14, a reduction in cell viability was found at concentrations an order of magnitude higher than the IC_{50}, whereas BC12 and BC14 had no effect at all concentrations tested, up to and including 100 μM (Figure 5C). Blasticidin (10 μg/mL) and DMSO (10% v/v) reduced cell viability in the order of 45% and 90%, respectively.

DISCUSSION

Analysis of compounds identified as potential $K_{Na}1.1$ inhibitors by *in silico* docking yielded six previously unknown inhibitors, each more potent than quinidine that has been trialed clinically as a stratified treatment for *KCNT1*-associated epilepsy. These inhibitors are structurally diverse and there is no clear pharmacophore, although BC6 and BC7 are among the scaffolds with structural similarity to bepridil. We propose that each of these compounds, in addition to quinidine and bepridil, inhibits the channel by blocking the pore via the intracellular vestibule. This is indicated by the reduced efficacy of each compound with the F346S pore mutation, and which is likely to be independent of the increased channel activity caused by
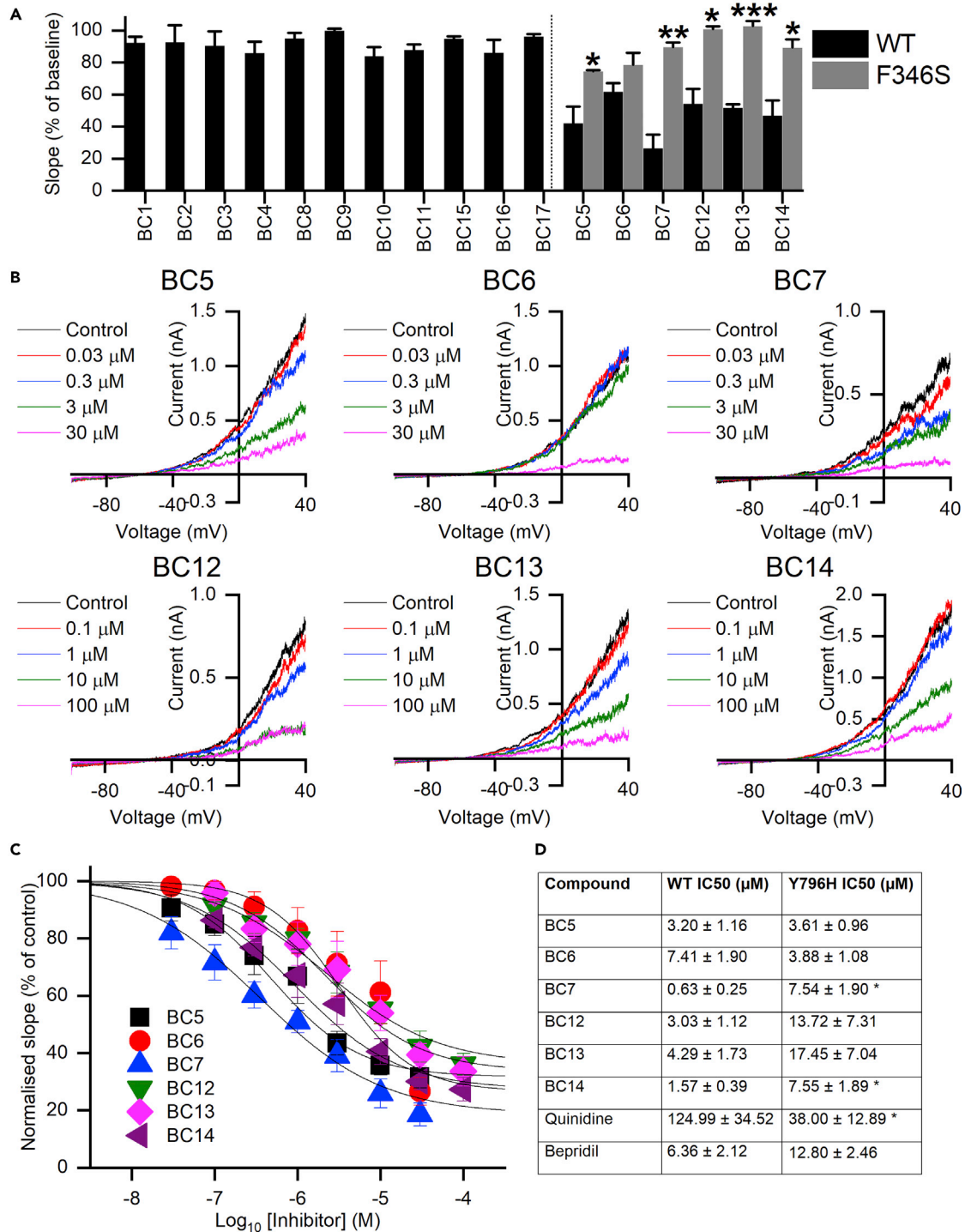
Figure 3. Functional Evaluation of Top-Scoring Molecules from *In Silico* Docking

(A) Mean (±SEM, n = 3–4 cells) WT $K_{Na}1.1$ conductance measured as the slope of the current evoked by depolarizing voltage ramps, relative to baseline, in the presence of 10 µM test compound; with those that were active (right of dashed line) counter-tested with F346S $K_{Na}1.1$ pore mutant (*p < 0.05, **p < 0.005, ***p < 0.0005, t test.).

(B and C) (B) Representative traces and (C) mean (±SEM, n = 5–7 cells) concentration-inhibition plots for active inhibitors.

(D) Summary table with mean (±SEM) potencies of compounds inhibiting WT and Y796H $K_{Na}1.1$ (n = 5–7 cells). *p < 0.05 versus potency with WT $K_{Na}1.1$ (Student t test).

See also Table S1, Figures S1 and S2.
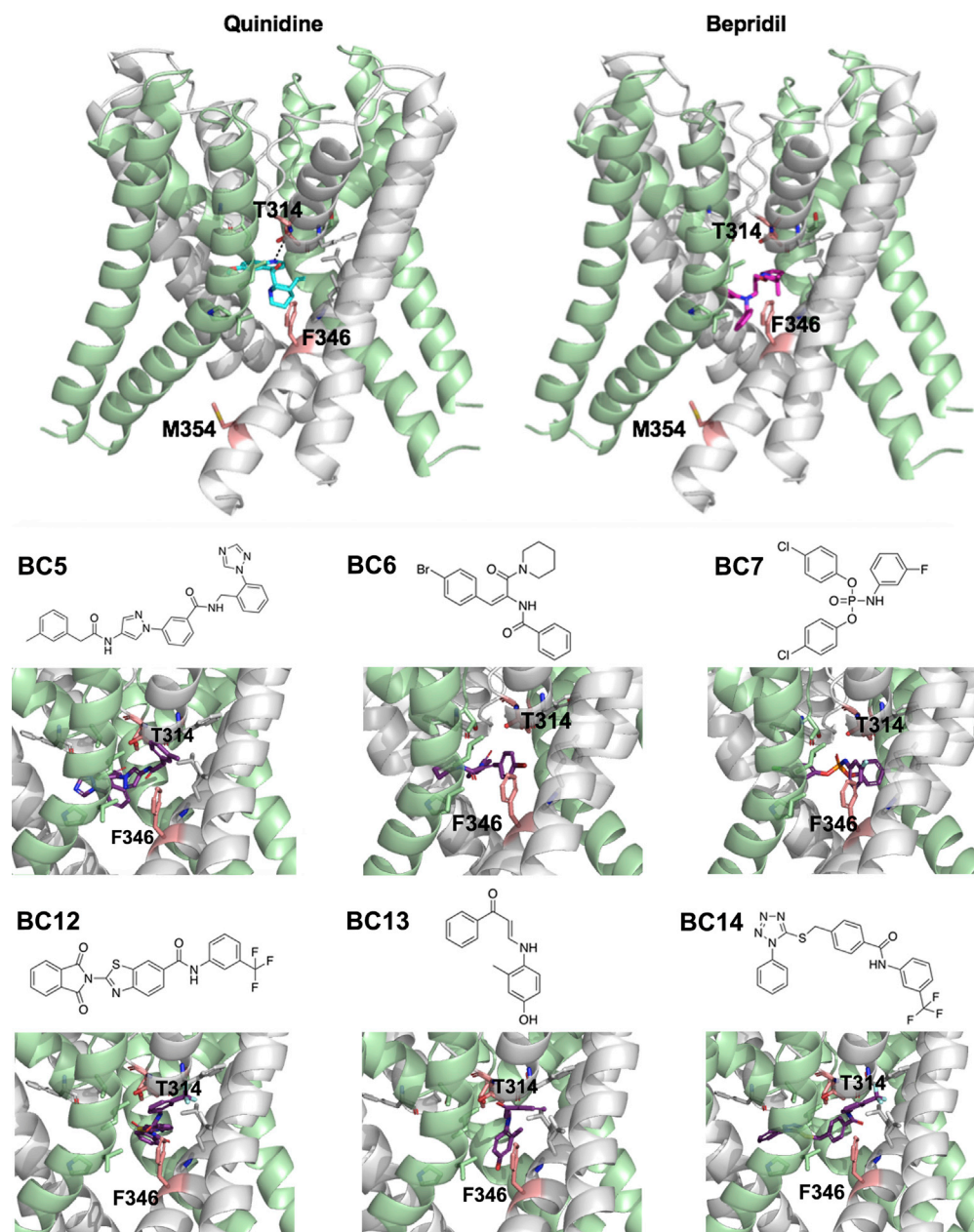
Figure 4. Chemical Structures of Inhibitors (Magenta) and Their Docked Poses in the $K_{Na}1.1$ Pore Domain

Side chains at positions equivalent to the human isoform are indicated (pink): T314 in the P loop and F346 and M354 in the S6 segment of human $K_{Na}1.1$. For clarity, the compounds are shown above each panel for the inhibitors analyzed in Figure 3.

the mutation, since with quinidine there was no similar loss of efficacy with Y796H, an epilepsy-causing mutation distal from the pore. The effects of mutations of F346 are somewhat modest, yielding a 10-fold decrease in potency, compared with WT $K_{Na}1.1$, suggesting that other interactions are necessary, but are consistent with the hypothesis that inhibitors block the channel by occupying the inner vestibule of the pore. This residue is also at the equivalent position in the S6 segment as F656 in hERG that co-ordinates inhibitor binding of quinidine, bepridil, and clofilium (Kamiya et al., 2006; Macdonald et al., 2018; Perry et al., 2004). This mode of action requires the inhibiting compound to traverse the plasma membrane and enter the pore via the cytoplasm. It is noteworthy that each of the compounds tested that had a
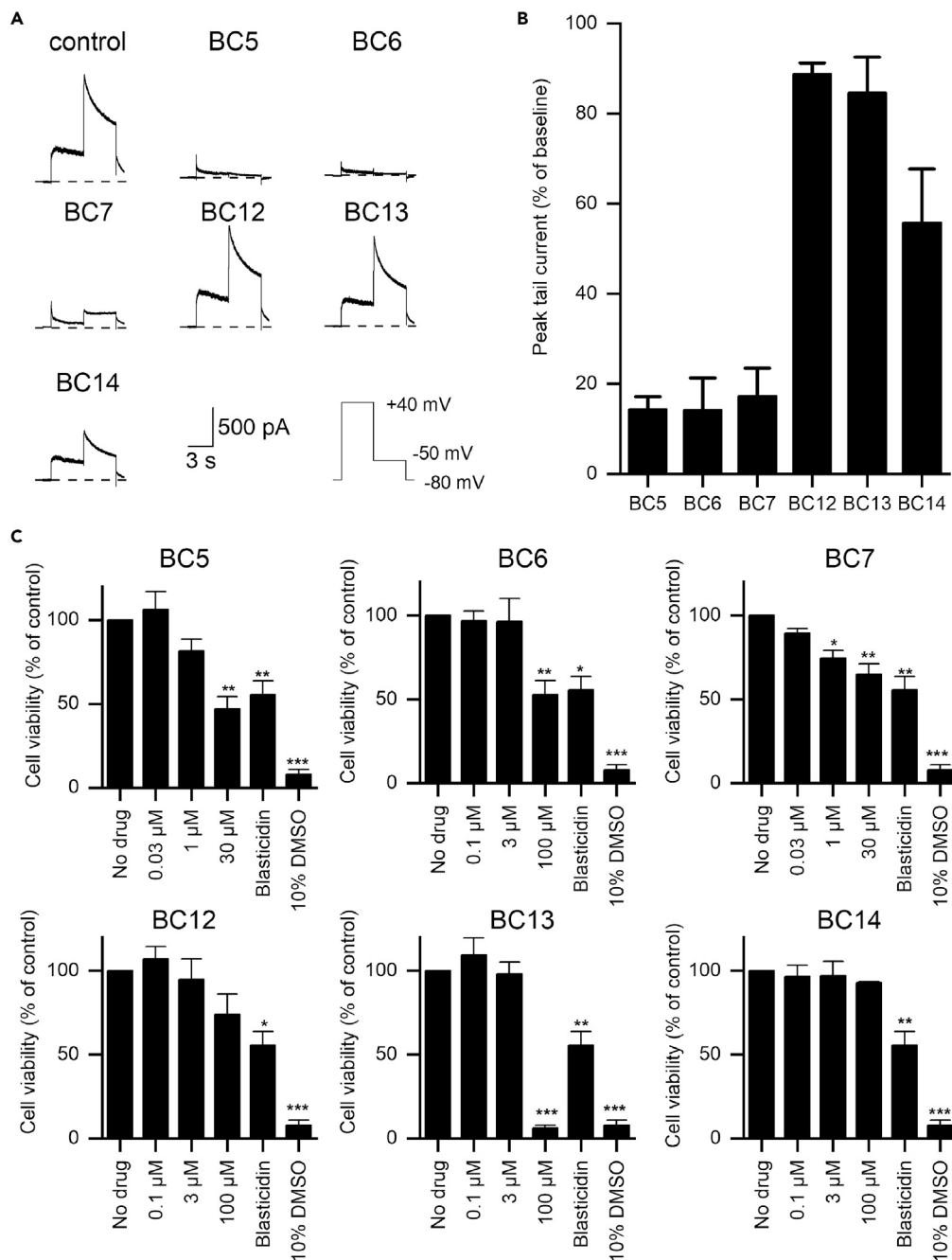
Figure 5. Preliminary Toxicological Assessment of $K_{Na}1.1$ Channel Inhibitors

(A) Representative hERG whole-cell currents recorded from a transfected HEK 293 cell in the absence (control) and presence of 10 μM inhibitor, as indicated.

(B) Mean (±SEM, n = 3) tail current at −50 mV remaining in the presence of each inhibitor.

(C) Cytotoxicity assays indicating mean (±SEM, n = 3) viability of HEK 293 cells using WST reagent following overnight exposure to inhibitor at the indicated concentrations, with 10 μM blasticidin and 10% v/v DMSO as positive controls; *p < 0.05, **p < 0.005, ***p < 0.0005, independent one-way ANOVA with Dunnett's post hoc test.

calculated logP (cLogP) value of 3.2 or less did not exhibit inhibition of $K_{Na}1.1$, and this may have been a result of poor membrane permeability. By using a model of the ion channel pore that is putatively in the open conformation, we had anticipated that inhibitors identified through docking would achieve similar or even higher potency with the Y796H mutant $K_{Na}1.1$, but this was not always the case. It is possible

that the apparent decrease in potency of some of the compounds with Y796H may be attributed to the high level of basal channel activity with this mutant channel and incomplete series resistance compensation. This could underestimate channel inhibition at the lower concentrations and increase variability. The increase in potency of quinidine with Y796H, relative to WT $K_{Na}1.1$, however, is consistent with previous studies of other gain-of-function mutations (Rizzo et al., 2016).

It may have been possible to obtain inhibitors by testing compounds identified through computational tools to have structures similar to the known inhibitors, quinidine, bepridil, and clofilium, but without using molecular docking. The risk with this approach is that the compounds may also have similar potency in inhibiting cardiac ion channels, which would preclude their further development. Indeed, this is what we found with BC6 and BC7, which both almost completely inhibited hERG currents at 10 μM. Instead, by docking a diverse library, we were able to identify compounds that were structurally distinct from the known inhibitors and that included some that had little effect on hERG at 10 μM. Together, this highlights the importance of screening a wide range of compounds, which in our approach employed virtual screening using computational approaches instead of a high-throughput cell-based functional screen. Other sites in the channel protein could potentially be used to target molecular docking and virtual screening, which may enhance $K_{Na}1.1$ selectivity over other ion channels, but there is presently a lack of understanding of how other $K_{Na}1.1$ domains could be targeted pharmacologically to modulate channel function.

Although the cryo-EM structures indicate that activation by sodium involves an expansion of the intracellular pore vestibule (Hite and MacKinnon, 2017), functional experiments with this and the closely related $K_{Na}1.2$ and $K_{Ca}1.1$ (BK_{Ca}) channels point to the selectivity filter and proximal hydrophobic residues, rather than an S6 helix bundle, as the location of the channel gate (Garg et al., 2013; Giese et al., 2017; Jia et al., 2018; Suzuki et al., 2016). This means that the inhibitors described here block at the channel gate and this should be a mode of inhibition that is efficacious with virtually all clinical gain-of-function mutations, independent of the mechanism by which increased open probability is achieved, rather than an inhibitor that binds to modulatory sites. An exception, however, may be F346L that was identified in a patient with EIMFS (McTague et al., 2018), which, based on our findings with mutations generated at this site in the pore, may have reduced inhibitor sensitivity. Indeed, it was found that F346L $K_{Na}1.1$ channels expressed in *Xenopus* oocytes were resistant to block by 300 μM quinidine (McTague et al., 2018), although the pharmacological effects of quinidine on channels containing a mixture of F346L and wild-type subunits, to mimic the heterozygous disorder, has not been explored.

Notwithstanding our preliminary efforts to characterize the potential toxicity of these inhibitors by studying inhibition of hERG channel currents and the effects in cell viability assays, we are unable to make any statement regarding their selectivity or safety ahead of any *in vitro* or *in vivo* investigation. Since the computational approach was based on the inhibition by quinidine and bepridil, one might expect a similar range of ion channels to be inhibited by the compounds described here. However, the low level of inhibition of hERG at 10 μM by BC12 and BC13 suggests that across the compounds there may be varying levels of selectivity, which could be further improved by synthesis and analysis of derivative compounds and testing their effects on a range of different cation channels. We do note, however, the characteristics of pan-assay interference (PAINS) in compounds BC6, BC7, and BC13, owing to the presence of the conjugated carbonyl group, meaning there may be non-specific effects in other functional assays. The lack of effects of the four analogues of BC12 tested demonstrates the potential for generating an inhibitor pharmacophore from this compound; thus, these may provide starting points for the development of more potent inhibitors.

The generation of high-resolution structural data by cryo-electron microscopy and single particle analysis has had a significant impact in structural biology. Importantly, circumventing the need to crystallize samples means that membrane proteins are more amenable to analysis, and also that human proteins, rather than homologs from prokaryotes and lower eukaryotes, now feature more prominently. This means that, for *in silico* analysis and drug discovery, target proteins very close to human, if not the human protein itself, can be utilized. The pore domain of the chicken $K_{Na}1.1$ subunit, however, is virtually identical to that of the human homolog, and we demonstrate its suitability for *in silico* docking experiments to provide potential inhibitors to characterize using a functional assay. Our study, in addition to identifying $K_{Na}1.1$ inhibitors from a compound library, provides a further example of the use of cryo-electron microscopy-generated membrane protein structural data in identifying new small molecule inhibitors through a structure-based discovery approach.

Limitations of the Study

A structure of the human $K_{Na}1.1$ channel was not available, so we employed that of the chicken homolog. The channel domain used for the docking experiments is highly conserved between chicken and human $K_{Na}1.1$, and the specific residues discussed are conserved. By restricting the docking experiments to the intracellular pore vestibule of the channel, to decrease computational complexity, we disregarded potential interactions of compounds with other parts of the protein.

RESOURCE AVAILABILITY

Lead Contact

Further information and requests for resources and reagents should be directed to and will be fulfilled by the Lead Contact, Dr Jonathan Lippiat (j.d.lippiat@leeds.ac.uk).

Material Availability

Plasmids generated in this study will be made available on request, but we may require a payment and/or a completed Materials Transfer Agreement if there is potential for commercial application.

Data and Code Availability

Raw data will be shared upon receipt of a reasonable request.

METHODS

All methods can be found in the accompanying Transparent Methods supplemental file.

SUPPLEMENTAL INFORMATION

Supplemental Information can be found online at https://doi.org/10.1016/j.isci.2020.101100.

AUTHOR CONTRIBUTIONS

J.D.L., S.P.M, B.A.C., and R.M.J. conceptualized the project, created figures, and wrote the initial draft of the manuscript. B.A.C, R.M.J, H.D., and J.D.L. generated new resources, conducted experimental investigation, and conducted analysis. J.D.L., S.P.M., C.W.G.F., and N.P. supervised the research. All authors reviewed and edited the manuscript.

DECLARATION OF INTERESTS

The authors declare no competing interests.

REFERENCES

Barcia, G., Fleming, M.R., Deligniere, A., Gazula, V.R., Brown, M.R., Langouet, M., Chen, H., Kronengold, J., Abhyankar, A., Cilio, R., et al. (2012). De novo gain-of-function KCNT1 channel mutations cause malignant migrating partial seizures of infancy. Nat. Genet. *44*, 1255–1259.

Bhattacharjee, A., Gan, L., and Kaczmarek, L.K. (2002). Localization of the Slack potassium channel in the rat central nervous system. J. Comp. Neurol. *454*, 241–254.

Budelli, G., Hage, T.A., Wei, A., Rojas, P., Jong, Y.J., O'Malley, K., and Salkoff, L. (2009). Na+-activated K+ channels express a large delayed outward current in neurons during normal physiology. Nat. Neurosci. *12*, 745–750.

Cataldi, M., Nobili, L., Zara, F., Combi, R., Prato, G., Giacomini, T., Capra, V., De Marco, P., Ferini-Strambi, L., and Mancardi, M.M. (2019). Migrating focal seizures in autosomal dominant sleep-related hypermotor epilepsy with KCNT1 mutation. Seizure *67*, 57–60.

Cervantes, B., Vega, R., Limon, A., and Soto, E. (2013). Identity, expression and functional role of the sodium-activated potassium current in vestibular ganglion afferent neurons. Neuroscience *240*, 163–175.

Chong, P.F., Nakamura, R., Saitsu, H., Matsumoto, N., and Kira, R. (2016). Ineffective quinidine therapy in early onset epileptic encephalopathy with KCNT1 mutation. Ann. Neurol. *79*, 502–503.

de Los Angeles Tejada, M., Stolpe, K., Meinild, A.K., and Klaerke, D.A. (2012). Clofilium inhibits Slick and Slack potassium channels. Biologics 6, 465–470.

Fitzgerald, M.P., Fiannacca, M., Smith, D.M., Gertler, T.S., Gunning, B., Syrbe, S., Verbeek, N., Stamberger, H., Weckhuysen, S., Ceulemans, B., et al. (2019). Treatment responsiveness in KCNT1-related epilepsy. Neurotherapeutics 16, 848–857.

Garg, P., Gardner, A., Garg, V., and Sanguinetti, M.C. (2013). Structural basis of ion permeation gating in Slo2.1 K+ channels. J. Gen. Physiol. 142, 523–542.

Gertler, T., Bearden, D., Bhattacharjee, A., and Carvill, G. (2018). KCNT1-related epilepsy. In GeneReviews((R)) [Internet], M.P. Adam, H.H. Ardinger, R.A. Pagon, S.E. Wallace, L.J.H. Bean, K. Stephens, and A. Amemiya, eds. (University of Washington, Seattle). https://pubmed.ncbi.nlm.nih.gov/30234941/.

Giese, M.H., Gardner, A., Hansen, A., and Sanguinetti, M.C. (2017). Molecular mechanisms of Slo2 K(+) channel closure. J. Physiol. 595, 2321–2336.

Hage, T.A., and Salkoff, L. (2012). Sodium-activated potassium channels are functionally coupled to persistent sodium currents. J. Neurosci. 32, 2714–2721.

Heron, S.E., Smith, K.R., Bahlo, M., Nobili, L., Kahana, E., Licchetta, L., Oliver, K.L., Mazarib, A., Afawi, Z., Korczyn, A., et al. (2012). Missense mutations in the sodium-gated potassium channel gene KCNT1 cause severe autosomal dominant nocturnal frontal lobe epilepsy. Nat. Genet. 44, 1188–1190.

Hite, R.K., and MacKinnon, R. (2017). Structural titration of Slo2.2, a Na(+)-dependent K(+) channel. Cell 168, 390–399.e11.

Hite, R.K., Yuan, P., Li, Z., Hsuing, Y., Walz, T., and MacKinnon, R. (2015). Cryo-electron microscopy structure of the Slo2.2 Na(+)-activated K(+) channel. Nature 527, 198–203.

Jia, Y., Lin, Y., Li, J., Li, M., Zhang, Y., Hou, Y., Liu, A., Zhang, L., Li, L., Xiang, P., et al. (2019). Quinidine therapy for lennox-gastaut syndrome with KCNT1 mutation. a case report and literature review. Front. Neurol. 10, 64.

Jia, Z., Yazdani, M., Zhang, G., Cui, J., and Chen, J. (2018). Hydrophobic gating in BK channels. Nat. Commun. 9, 3408.

Joiner, W.J., Tang, M.D., Wang, L.Y., Dworetzky, S.I., Boissard, C.G., Gan, L., Gribkoff, V.K., and Kaczmarek, L.K. (1998). Formation of intermediate-conductance calcium-activated potassium channels by interaction of Slack and Slo subunits. Nat. Neurosci. 1, 462–469.

Kamiya, K., Niwa, R., Mitcheson, J.S., and Sanguinetti, M.C. (2006). Molecular determinants of HERG channel block. Mol. Pharmacol. 69, 1709–1716.

Knape, K., Linder, T., Wolschann, P., Beyer, A., and Stary-Weinzinger, A. (2011). In silico analysis of conformational changes induced by mutation of aromatic binding residues: consequences for drug binding in the hERG K+ channel. PLoS One 6, e28778.

Lim, C.X., Ricos, M.G., Dibbens, L.M., and Heron, S.E. (2016). KCNT1 mutations in seizure disorders: the phenotypic spectrum and functional effects. J. Med. Genet. 53, 217–225.

Lin, X., Li, X., and Lin, X. (2020). A review on applications of computational methods in drug screening and design. Molecules 25, 1375.

Liu, X., and Stan Leung, L. (2004). Sodium-activated potassium conductance participates in the depolarizing afterpotential following a single action potential in rat hippocampal CA1 pyramidal cells. Brain Res. 1023, 185–192.

Macdonald, L.C., Kim, R.Y., Kurata, H.T., and Fedida, D. (2018). Probing the molecular basis of hERG drug block with unnatural amino acids. Sci. Rep. 8, 289.

Madaan, P., Jauhari, P., Gupta, A., Chakrabarty, B., and Gulati, S. (2018). A quinidine non responsive novel KCNT1 mutation in an Indian infant with epilepsy of infancy with migrating focal seizures. Brain Dev. 40, 229–232.

Martin, H.C., Kim, G.E., Pagnamenta, A.T., Murakami, Y., Carvill, G.L., Meyer, E., Copley, R.R., Rimmer, A., Barcia, G., Fleming, M.R., et al. (2014). Clinical whole-genome sequencing in severe early-onset epilepsy reveals new genes and improves molecular diagnosis. Hum. Mol. Genet. 23, 3200–3211.

McTague, A., Nair, U., Malhotra, S., Meyer, E., Trump, N., Gazina, E.V., Papandreou, A., Ngoh, A., Ackermann, S., Ambegaonkar, G., et al. (2018). Clinical and molecular characterization of KCNT1-related severe early-onset epilepsy. Neurology 90, e55–e66.

Mikati, M.A., Jiang, Y.H., Carboni, M., Shashi, V., Petrovski, S., Spillmann, R., Milligan, C.J., Li, M., Grefe, A., McConkie, A., et al. (2015). Quinidine in the treatment of KCNT1-positive epilepsies. Ann. Neurol. 78, 995–999.

Milligan, C.J., Li, M., Gazina, E.V., Heron, S.E., Nair, U., Trager, C., Reid, C.A., Venkat, A., Younkin, D.P., Dlugos, D.J., et al. (2014). KCNT1 gain of function in 2 epilepsy phenotypes is reversed by quinidine. Ann. Neurol. 75, 581–590.

Mullen, S.A., Carney, P.W., Roten, A., Ching, M., Lightfoot, P.A., Churilov, L., Nair, U., Li, M., Berkovic, S.F., Petrou, S., et al. (2018). Precision therapy for epilepsy due to KCNT1 mutations: a randomized trial of oral quinidine. Neurology 90, e67–e72.

Nanou, E., Kyriakatos, A., Bhattacharjee, A., Kaczmarek, L.K., Paratcha, G., and El Manira, A. (2008). Na+-mediated coupling between AMPA receptors and KNa channels shapes synaptic transmission. Proc. Natl. Acad. Sci. U S A. 105, 20941–20946.

Ohba, C., Kato, M., Takahashi, N., Osaka, H., Shiihara, T., Tohyama, J., Nabatame, S., Azuma, J., Fujii, Y., Hara, M., et al. (2015). De novo KCNT1 mutations in early-onset epileptic encephalopathy. Epilepsia 56, e121–e128.

Perry, M., de Groot, M.J., Helliwell, R., Leishman, D., Tristani-Firouzi, M., Sanguinetti, M.C., and Mitcheson, J. (2004). Structural determinants of HERG channel block by clofilium and ibutilide. Mol. Pharmacol. 66, 240–249.

Quraishi, I.H., Stern, S., Mangan, K.P., Zhang, Y., Ali, S.R., Mercier, M.R., Marchetto, M.C., McLachlan, M.J., Jones, E.M., Gage, F.H., et al. (2019). An epilepsy-associated KCNT1 mutation enhances excitability of human iPSC-derived neurons by increasing Slack KNa currents. J. Neurosci. 39, 7438–7449.

Rawson, S., Davies, S., Lippiat, J.D., and Muench, S.P. (2016). The changing landscape of membrane protein structural biology through developments in electron microscopy. Mol. Membr. Biol. 33, 12–22.

Rizzi, S., Knaus, H.G., and Schwarzer, C. (2016). Differential distribution of the sodium-activated potassium channels slick and slack in mouse brain. J. Comp. Neurol. 524, 2093–2116.

Rizzo, F., Ambrosino, P., Guacci, A., Chetta, M., Marchese, G., Rocco, T., Soldovieri, M.V., Manocchio, L., Mosca, I., Casara, G., et al. (2016). Characterization of two de novoKCNT1 mutations in children with malignant migrating partial seizures in infancy. Mol. Cell Neurosci. 72, 54–63.

Rubboli, G., Plazzi, G., Picard, F., Nobili, L., Hirsch, E., Chelly, J., Prayson, R.A., Boutonnat, J., Bramerio, M., Kahane, P., et al. (2019). Mild malformations of cortical development in sleep-related hypermotor epilepsy due to KCNT1 mutations. Ann. Clin. Transl. Neurol. 6, 386–391.

Suzuki, T., Hansen, A., and Sanguinetti, M.C. (2016). Hydrophobic interactions between the S5 segment and the pore helix stabilizes the closed state of Slo2.1 potassium channels. Biochim. Biophys. Acta 1858, 783–792.

Swinney, D.C., and Xia, S. (2014). The discovery of medicines for rare diseases. Future Med. Chem. 6, 987–1002.

Wrighton, D.C., Muench, S.P., and Lippiat, J.D. (2015). Mechanism of inhibition of mouse Slo3 (KCa 5.1) potassium channels by quinine, quinidine and barium. Br. J. Pharmacol. 172, 4355–4363.

Yang, B., Gribkoff, V.K., Pan, J., Damagnez, V., Dworetzky, S.I., Boissard, C.G., Bhattacharjee, A., Yan, Y., Sigworth, F.J., and Kaczmarek, L.K. (2006). Pharmacological activation and inhibition of Slack (Slo2.2) channels. Neuropharmacology 51, 896–906.

Yuan, A., Santi, C.M., Wei, A., Wang, Z.W., Pollak, K., Nonet, M., Kaczmarek, L., Crowder, C.M., and Salkoff, L. (2003). The sodium-activated potassium channel is encoded by a member of the Slo gene family. Neuron 37, 765–773.

Supplemental Information

Structure-Based Identification and Characterization

of Inhibitors of the Epilepsy-Associated

K$_{Na}$1.1 (KCNT1) Potassium Channel

Bethan A. Cole, Rachel M. Johnson, Hattapark Dejakaisaya, Nadia Pilati, Colin W.G. Fishwick, Stephen P. Muench, and Jonathan D. Lippiat

Table S1. Details of compounds tested, Related to Figures 3 and 4: Top-scoring compounds identified through virtual high-throughput screening or #bepridil overlay, assessed for $K_{Na}1.1$ inhibition at 10 µM. *Compounds that demonstrated >40% inhibition and were studied further. The predicted H-bonds use the amino acid sequence in the chicken $K_{Na}1.1$ structure (PDB: 5U70), with corresponding positions in human $K_{Na}1.1$ in parentheses.

BC ID	PubChem ID	Chembridge ID	M.W.	cLogP	Docking score	Predicted H-bond
1	42211371	10226003	433.5	2.1	-8.731	E326 (E347) T293 (T314) x2
2	42170356	18717381	450.5	2.611	-8.841	T293 (T314) S392 (S313)
3	45198665	32500723	489.5	1.76	-9.151	T293 (T314) x2
4	72869676	38250229	360.4	2.9	-8.88	T293 (T314) x2
5*	42481567	38627778	491.5	4.154	-9.607	T293 (T314) F291 (F312)
6#*	1283470	5143781	413.3	4.81	-7.44	T293 (T314)
7#*	2272824	5214461	412.2	7.05	-7.189	T293 (T314) x2
8#	1376211	5422905	359.5	6.26	-7.246	n/a
9#	5341073	5574034	423.3	6.67	-7.28	T293 (T314)
10	5342180	5690314	459.5	6.64	-9.022	F291 (F312) T293 (T314) x2
11	56902153	60526468	324.4	3.21	-9.074	F291 (F312)
12*	1330052	7040211	467.4	5.37	-8.732	F291 (F312) T293 (T314) x2
13*	2185932	7364411	253.3	3.906	-8.891	F291
14*	1243440	7942343	455.5	5.214	-8.891	n/a
15	72922744	84082349	359.4	1.15	-8.638	F291 (F312) T293 (T314) x2
16	70780443	90931265	327.4	1.83	-8.74	F291 (F312)
17	25249672	9273389	260.4	3.085	-8.861	F291 (F312)
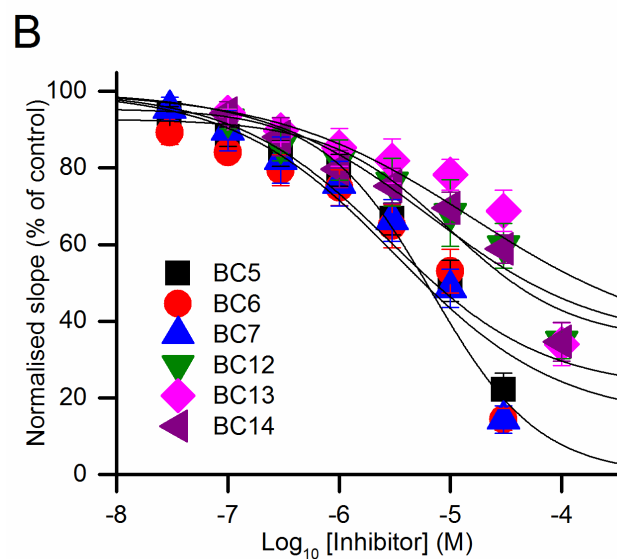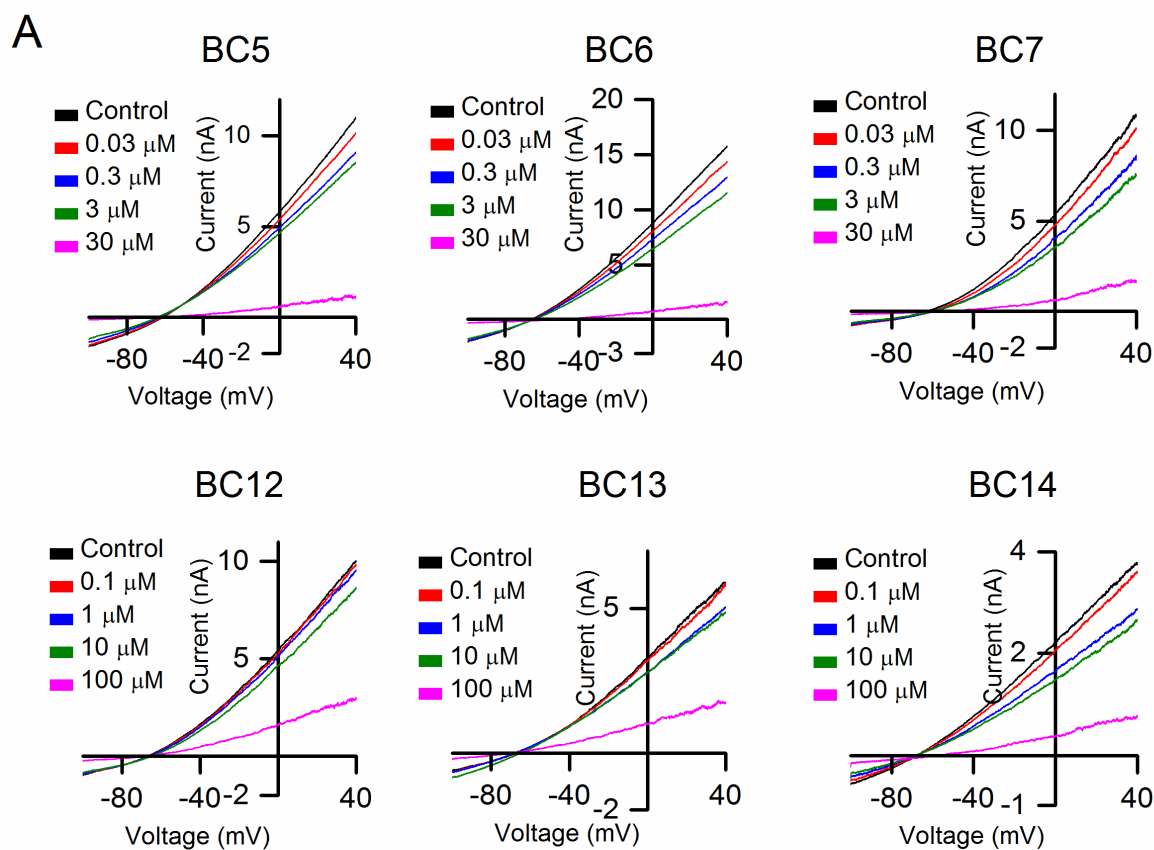
Figure S1. Functional evaluation of novel inhibitors with K$_{Na}$1.1 channels harbouring the epilepsy-causing mutation Y796H, Related to Figure 3. **A** Representative traces and **B** mean (± SEM, n= 5 to 7 cells) concentration-inhibition plots for active inhibitors. **C** Mean (± SEM, n= 5 to 7 cells) potencies of compounds inhibiting Y796H K$_{Na}$1.1; quinidine data from Figure 2.
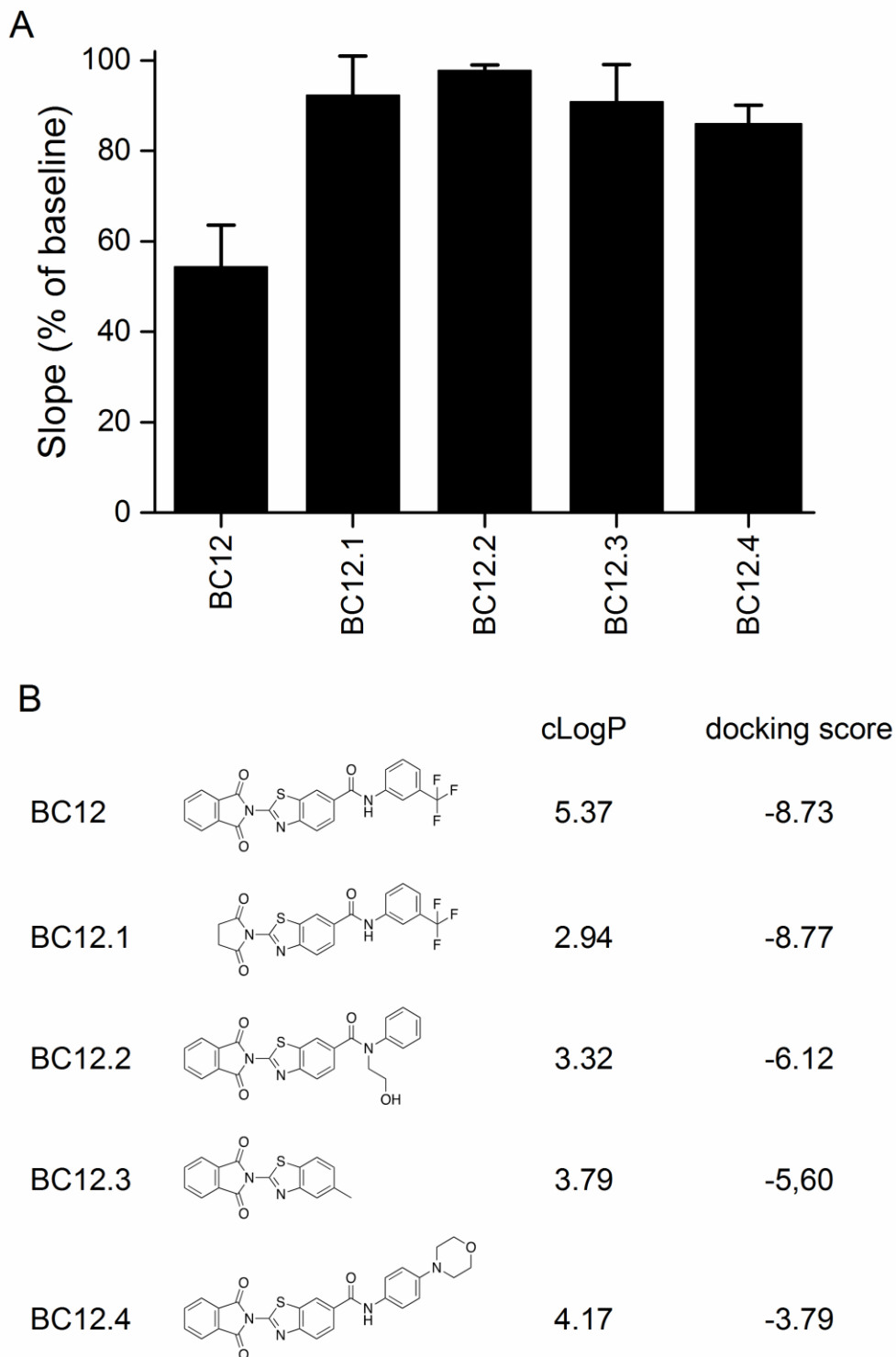
Figure S2: Evaluation of compounds simlar to BC12, Related to Figure 3. **A** Mean (± SEM, n = 3) $K_{Na}1.1$ conductance, measured as the slope of the current evoked by a depolarising voltage ramp in the presence of 10 μM test compound relative to control solution. **B** Chemical structures of compounds tested, their computed LogP (cLogP) and Glide docking score.

Transparent Methods

Model preparation and molecular docking

Models of the $K_{Na}1.1$ pore domain were generated in UCSF Chimera using the atomic models of the putative closed and open tetrameric channel conformations (PDB:5U76 and 5U70, respectively (Hite and MacKinnon, 2017)), and comprised residues 244 to 340 ($S^{244}AMF…LWME^{334}$) of each subunit. Automated docking was conducted using SwissDock (Grosdidier et al., 2011) and GLIDE (Friesner et al., 2004) in Maestro (Schrödinger). With SwissDock, docking of quinidine and bepridil was carried out using the entire model of the pore domain. Virtual high-throughput screening was performed using GLIDE with the model of the pore domain in the putative open conformation, targeting a 20 x 20 x 20 Å square box that enclosed side chains from both the selectivity filter and S6 transmembrane segment that line the intracellular pore vestibule. Both protein and ligand-based docking approaches were used. Initially, a Chembridge library consisting of 100,000 drug-like screening compounds were screened in HTVS mode, ranked according to their predicted binding affinities, and the top-scoring 10,000 compounds were then docked using the higher precision SP mode. Approximately 100 top-scoring compounds were visually inspected using PyMOL to identify the binding interactions with the protein. For the ligand-based approach, ROCS (Hawkins et al., 2007) was used to overlay the Chembridge library of compounds over the predicted bepridil binding pose. Compounds that were predicted to overlay with bepridil were subsequently docked, as above, into the inner pore vestibule and were analysed to determine whether they would form interactions with the protein. The structures of the best scoring compounds from both approaches were analysed to determine the 'drug-like' properties of the molecules. Of the top-scoring compounds which fit the criteria, 17 were ordered from Chembridge (Chembridge Corp., San Diego, CA) and were shipped as dry stocks in 1 or 5 mg quantities before being dissolved in dimethylsulphoxide to stock concentration of 10 mM.

Molecular biology and cell culture

A full-length $K_{Na}1.1$ cDNA clone (IMAGE: 9054424; Genbank BC171770.1) was obtained (Source Bioscience, Nottingham, U.K.) and the coding region subcloned into the pcDNA6-V5/His6 vector (Invitrogen). Mutations were introduced by the polymerase chain reaction using the New England

BioLabs mutagenesis method and confirmed by sequencing (Genewiz, Takeley, U.K.). Due to the large size and high GC content of the insert, some mutations were generated in a plasmid containing the Bsu36I/BspEI (pore mutants) or SbfI/BsiWI (Y796H) restriction fragment, and then subcloned into the corresponding sites in the pcDNA6-K_{Na}1.1 construct. Human embryonic kidney (HEK 293) cells were cultured in Dulbecco's modified Eagle medium (DMEM with GlutaMax, Invitrogen), supplemented with 10% v/v foetal bovine serum, 50 U/ml penicillin, and 0.05 mg/ml streptomycin. Cells were co-transfected with pcDNA6-K_{Na}1.1 and pEYFP-N1 plasmid DNA using Mirus TransIT-X2 reagent (Geneflow, Lichfield, U.K.) and were plated onto borosilicate glass cover slips for electrophysiological experiments, which were conducted 2 to 4 days later.

Electrophysiology

Unless otherwise stated, all chemicals were obtained from Sigma-Aldrich (Gillingham, U.K.). Patch pipettes were pulled from thin-walled borosilicate glass (Harvard Apparatus Ltd, Edenbridge, Kent, UK), polished, and gave resistances of 1.5 to 2.5 MΩ in the experimental solutions. The pipette solution contained, in mM, 100 K-Gluconate, 30 KCl, 10 Na-Gluconate, 29 Glucose, 5 EGTA and 10 HEPES, pH 7.3 with KOH and the bath solution contained, in mM, 140 NaCl, 1 $CaCl_2$, 5 KCl, 29 Glucose, 10 HEPES and 1 $MgCl_2$, pH 7.4 with NaOH. Currents were recorded from fluorescing cells at room temperature (20 to 22 °C) using the whole-cell patch clamp configuration using an EPC-10 amplifier (HEKA Electronics, Lambrecht, Germany), with >65 % series resistance compensation (where appropriate), 2.9 kHz low-pass filtering, and 10 kHz digitisation. For current-voltage analysis, cells were held at -80 mV and 400 ms pulses were applied to voltages between -100 and 80 mV. To evaluate inhibition by compounds, cells were held at -80 mV and 500 ms voltage ramps were applied from -100 to 40 mV at 0.2 Hz. Initially compounds, which were delivered by gravity perfusion, were applied serially at 10 µM (0.1 % final DMSO content) for 2 min, followed by at least 2 min wash with control solution before the next compound was added. Those compounds that that exhibited at least 40% current inhibition were analysed further by concentration-inhibition analysis: $G/G_C = (1 + ([B]/IC_{50})^H)^{-1} + c$, where G is the conductance measured as the slope of the current evoked by the voltage ramp in the presence of the inhibitor, I_C is the control conductance in the absence of inhibitor, [B] is the concentration of the inhibitor, IC_{50} the concentration of inhibitor that yields 50% inhibition, H the slope factor, and c the residual current. For hERG currents, cells were held at -80 mV and 4 s depolarising pulses to +40 and then -50 mV were applied at 0.2 Hz. Data were analysed using Fitmaster (HEKA Electronics, Lambrecht, Germany), Microsoft Excel, and OriginPro 7.5 (OriginLab

Corporation, Northampton, MA, USA). Data are presented as means ± SEM (n = number of cells). Statistical analysis was carried out using SPSS (IBM analytics, Portsmouth, UK) with $p < 0.05$ being considered significant.

Cytotoxicity assay

Non-transfected HEK 293 cells were seeded at a density of 5×10^4 cells/ well in culture medium in a 96-well plate and incubated overnight at 37 °C in 5% CO_2. Following exposure to three different concentrations of inhibitor for 24 hours, WST-1 reagent (Source Bioscience, Nottingham, U.K.) was added and cells were incubated for a further 2 hours. Inhibitor concentration ranges were selected to make comparison with effects on $K_{Na}1.1$ currents. Cells were also treated with 10% v/v DMSO or 10 µg/ml blasticidin as positive controls. Absorbance at 450 nm (reference 650 nm) was measured using the Flexstation 3 microplate reader (Molecular Devices, Wokingham, UK). Cell viability was calculated as a percentage of the absorbance measured from untreated cells. Data were analysed using Microsoft Excel and OriginPro 7.5 (OriginLab Corporation, Northampton, MA, USA). Data are presented as mean ± SEM (n = number of independent experiments). Statistical analysis was carried out using SPSS. Data were compared using an independent one-way ANOVA with Dunnett's post-hoc test; $p < 0.05$ was considered significant.

Supplementary References

Friesner, R.A., Banks, J.L., Murphy, R.B., Halgren, T.A., Klicic, J.J., Mainz, D.T., Repasky, M.P., Knoll, E.H., Shelley, M., Perry, J.K.*, et al.* (2004). Glide: a new approach for rapid, accurate docking and scoring. 1. Method and assessment of docking accuracy. J Med Chem *47*, 1739-1749.

Grosdidier, A., Zoete, V., and Michielin, O. (2011). SwissDock, a protein-small molecule docking web service based on EADock DSS. Nucleic Acids Res *39*, W270-277.

Hawkins, P.C., Skillman, A.G., and Nicholls, A. (2007). Comparison of shape-matching and docking as virtual screening tools. J Med Chem *50*, 74-82.

Hite, R.K., and MacKinnon, R. (2017). Structural Titration of Slo2.2, a Na(+)-Dependent K(+) Channel. Cell *168*, 390-399 e311.